BIOCHEMISTRY
including biophysical chemistry & molecular biology

ARTICLE

pubs.acs.org/biochemistry

Crystal Structures of Aspartate Aminotransferase Reconstituted with 1-Deazapyridoxal 5′-Phosphate: Internal Aldimine and Stable L-Aspartate External Aldimine

Wait R. Griswold, Andrew J. Fisher, and Michael D. Toney*

Department of Chemistry, University of California, One Shields Avenue, Davis, California 95616, United States

ABSTRACT: The 1.8 Å resolution crystal structures of *Escherichia coli* aspartate aminotransferase reconstituted with 1-deazapyridoxal 5′-phosphate (deazaPLP; 2-formyl-3-hydroxy-4-methylbenzyl phosphate) in the internal aldimine and L-aspartate external aldimine forms are reported. The L-aspartate·deazaPLP external aldimine is extraordinarily stable (half-life of >20 days), allowing crystals of this intermediate to be grown by cocrystallization with L-aspartate. This structure is compared to that of the α-methyl-L-aspartate·PLP external aldimine. Overlays with the corresponding pyridoxal 5′-phosphate (PLP) aldimines show very similar orientations of deazaPLP with respect to PLP. The lack of a hydrogen bond between Asp222 and deazaPLP, which serves to "anchor" PLP in the active site, releases strain in the deazaPLP internal aldimine that is enforced in the PLP internal aldimine [Hayashi, H., Mizuguchi, H., Miyahara, I., Islam, M. M., Ikushiro, H., Nakajima, Y., Hirotsu, K., and Kagamiyama, H. (2003) *Biochim. Biophys. Acta 1647*, 103] as evidenced by the planarity of the pyridine ring and the Schiff base linkage with Lys258. Additionally, loss of this anchor causes a 10° greater tilt of deazaPLP toward the substrate in the external aldimine. An important mechanistic difference between the L-aspartate·deazaPLP and α-methyl-L-aspartate·PLP external aldimines is a hydrogen bond between Gly38 and Lys258 in the former, positioning the catalytic base above and approximately equidistant between Cα and C4′. In contrast, in the α-methyl-L-aspartate·PLP external aldimine, the ε-amino group of Lys258 is rotated ∼70° to form a hydrogen bond to Tyr70 because of the steric bulk of the methyl group.

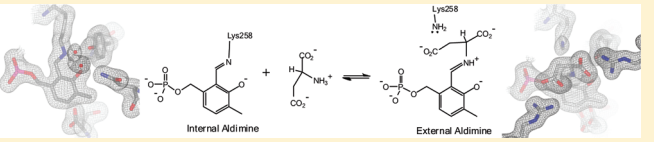

Pyridoxal 5′-phosphate (PLP) enzymes are unequaled in the variety of reaction types they catalyze, allowed by the cofactor's ability to resonance stabilize carbanionic intermediates (Figure 1A).[1−3] Indeed, considering the nearly universal invocation of the quinonoid resonance form of carbanionic intermediates in PLP enzyme mechanisms, one would expect that all enzymes allow the full potential of the electron sink by protonation of the pyridine ring. However, this is not the case. The X-ray structures of several PLP enzymes implicate different pyridine ring protonation states.[4−6]

At one extreme, aspartate aminotransferase (AAT), a representative fold type I enzyme, has an aspartic acid residue (Asp222; solution $pK_a \sim 4$) that fully protonates the pyridine nitrogen (solution $pK_a \sim 6.3$ as a Schiff base[7]) of PLP[8] to form a salt bridge[9] (Figure 1B). In the middle is alanine racemase (ALR), a fold type III enzyme, which has a positively charged arginine residue (Arg219; solution $pK_a \sim 13$) that forms a hydrogen bond to the pyridine N.[5] At the other extreme are enzymes like *O*-acetylserine sulfhydrylase (OASS), a fold type II enzyme with a serine residue (Ser272; solution $pK_a \sim 15$) that forms a hydrogen bond to the pyridine N.[6] This interaction between the pyridine ring and a serine residue is likely to leave the pyridine nitrogen unprotonated (Figure 1B).

Recent experimental and computational studies indicate that the protonated imino group of the external aldimine intermediate, through electrostatic and resonance stabilization of the carbanion (Figure 1A), plays a primary role in catalysis.[1,10−13] We synthesized an isosteric carbocyclic analogue of PLP, 1-deazapyridoxal 5′-phosphate (deazaPLP), to determine the extent to which various PLP enzymes require the electron sink properties of the pyridine ring.[14] DeazaPLP, lacking both the potential for protonation and the greater electronegativity of nitrogen versus carbon in the aromatic ring, is expected to be a very poor cofactor with fold type I enzymes, and less poor with fold type II and III PLP enzymes. This prediction is true in the case of aspartate aminotansferase. We report here the crystal structures of the internal aldimine and the stable L-aspartate external aldimine of *Escherichia coli* AAT reconstituted with deazaPLP.

EXPERIMENTAL PROCEDURES

Materials. Ammonium sulfate, L-aspartate, acetic acid, sodium acetate, potassium phosphate (mono- and dibasic), sodium chloride, and ethylene glycol were from Fisher. Triethanolamine (TEA), HEPES buffer, Luria-Bertani broth (LB), carbenicillin, pyridoxal 5′-phosphate, lysozyme, and cysteinesulfinic acid were from Sigma. Q-Sepharose Fast Flow anion exchange resin was from GE Healthcare. DeazaPLP was synthesized as described previously.[14]

Received: March 23, 2011
Revised: May 23, 2011
Published: May 31, 2011

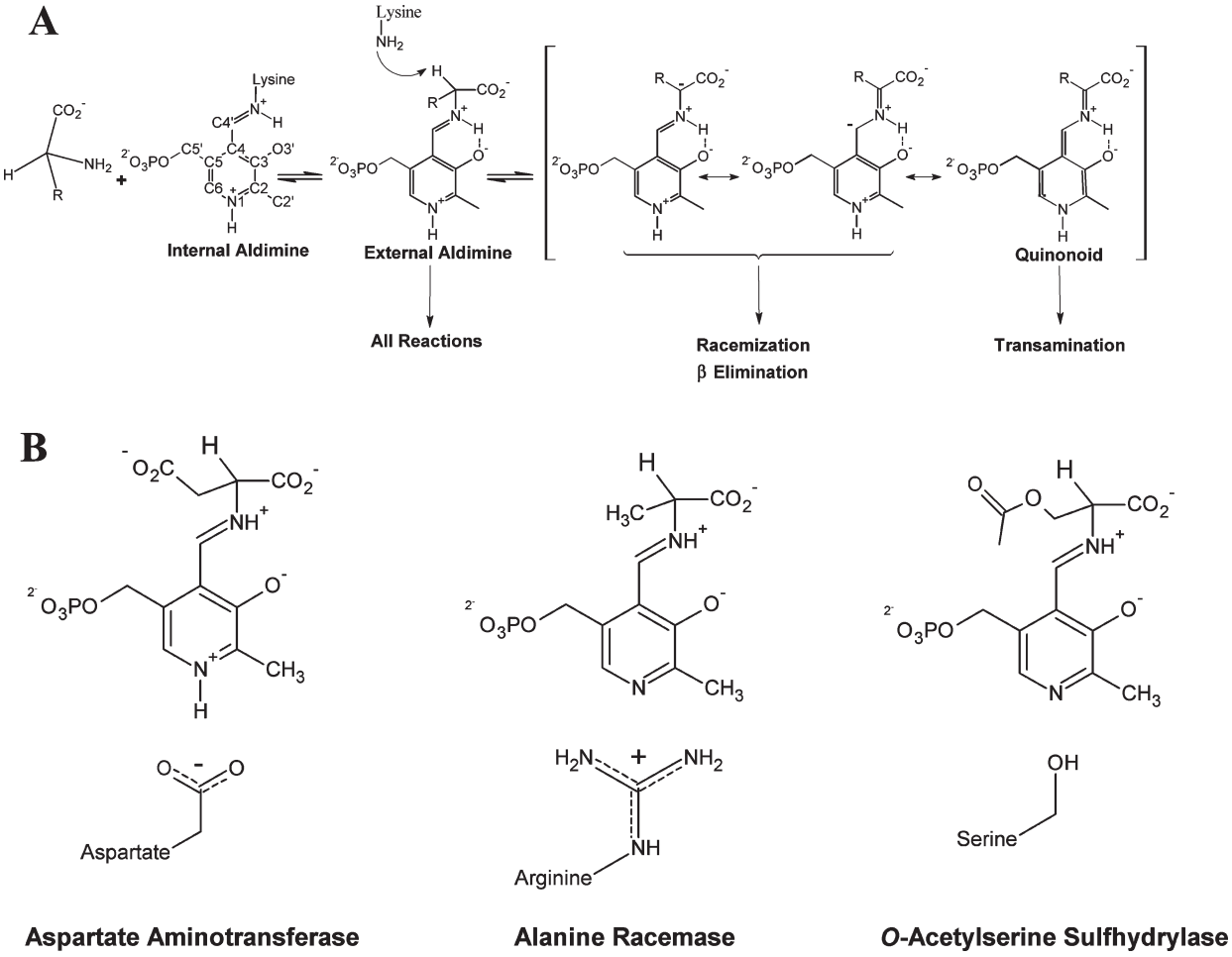

Figure 1. (A) Formation and stabilization of the carbanionic intermediate with a protonated pyridine nitrogen. The external aldimine is a common intermediate in all PLP-catalyzed reactions. (B) The protonation state of the pyridine nitrogen of PLP enzymes is expected to vary with the acidity of the amino acid side chain interacting with it. AAT is expected to fully protonate N1 of PLP via Asp222. Alanine racemase and *O*-acetylserine sulfhydrylase likely maintain N1 in a neutral state through interaction with Arg219 and Ser272, respectively.

Enzyme. A pUC119 plasmid containing the gene encoding *E. coli* AAT[15] was transformed into *E. coli* MG204 cells by electroporation. Transformed cells, grown on LB agar plates containing 100 μg/mL carbenicillin, were transferred to 2YT medium containing 100 μg/mL carbenicillin and grown with shaking at 225 rpm for 36 h at 37 °C. Cells were collected by centrifugation at 5000*g* for 30 min at 4 °C and were resuspended in lysis buffer [20 mM potassium phosphate buffer (pH 7.0), 200 μM PLP, and 0.5 mg/mL lysozyme]. The mixture was stirred on ice for 30 min then subjected to sonication, which consisted of five 1 min pulses performed for each 10 g of cell paste. The lysed cells were centrifuged at 18000*g* and 4 °C for 1 h. Sodium acetate was added to the supernatant to a final concentration of 20 mM and the pH lowered to 4.9 via the addition of dilute acetic acid. The resulting solution was cooled on ice for 10 min followed by centrifugation at 18000*g* for 30 min at 4 °C. The pellet, containing precipitated protein, was discarded, and the supernatant was dialyzed against three changes of 20 mM sodium acetate (pH 4.9) and 20 μM PLP. The dialysate was centrifuged at 12000*g* for 30 min at 4 °C, loaded at a rate of 2 mL/min onto a 50 mL Q-Sepharose Fast Flow anion exchange column, and washed with 10 bed volumes of wash buffer [20 mM sodium acetate (pH 4.9) and 20 μM PLP] at a rate of 4 mL/min. This was followed by a linear gradient elution from 100% wash buffer to 100% elution buffer [20 mM sodium acetate (pH 4.9), 300 mM NaCl, and 20 μM PLP] over 1 L at a flow rate of 2 mL/min. Fractions containing AAT, as judged by the absorbance at 430 nm, were analyzed by sodium dodecyl sulfate−polyacrylamide gel electrophoresis to assess purity. Pure fractions were combined, dialyzed against three changes of 20 mM HEPES (pH 7.5), and concentrated to 10 mg/mL. Aliquoted samples were flash-frozen in liquid nitrogen and stored at −80 °C. The apoenzyme was prepared as previously described[16] and reconstituted by overnight incubation with a 10-fold excess of deazaPLP. Dialysis was performed against 50 mm TEA (pH 7.5), 100 mM KCl, and 2 mM DTT to achieve a final free deazaPLP concentration of ∼10 μM followed by concentration of the enzyme to ∼15−20 mg/mL.

Crystallization and Data Collection. Crystals were obtained by the hanging drop method. A 2 μL drop of protein solution (15−20 mg/mL) [50 mM TEA (pH 7.5), 100 mM KCl, 2 mM DTT, and 10 μM deazaPLP] was mixed with 2 μL of reservoir buffer containing 53−60% saturated ammonium sulfate and 50 mM TEA (pH 7.5). L-Aspartate was added to a final concentration of 50 mM to the hanging drop to obtain the external aldimine. Large yellow crystals formed under the

dx.doi.org/10.1021/bi200436y |*Biochemistry* 2011, 50, 5918–5924

Table 1. Data Collection and Refinement Statistics for Deaza-PLP AAT Structures[a]

	internal aldimine	L-aspartate external aldimine
unit cell dimensions *a*, *b*, *c* (Å)	154.68, 84.75, 79.15	154.83, 83.78, 77.80
space group	$C222_1$	$C222_1$
no. of monomers per asymmetric unit	1	1
resolution range (Å)	77.3−1.80 (1.84−1.80)	38.9−1.80 (1.86−1.80)
R_{sym}[b] (%)	5.6 (42.8)	5.9 (39.6)
$\langle I\rangle/\sigma\langle I\rangle$	10.7 (2.2)	17.5 (2.8)
no. of reflections	167956 (11977)	160082 (15291)
no. of unique reflections	48807 (3603)	46701 (4606)
redundancy	3.4 (3.3)	3.4 (3.3)
completeness (%)	99.1 (99.7)	98.2 (97.5)
R_{factor}[c] (%)	15.15	14.79
R_{free}[d] (%)	18.80	17.90
no. of protein atoms	3151	3206
no. of cofactor atoms	15	24
no. of water atoms	396	323
no. of sulfate atoms	25	40
no. of ethylene glycol atoms	16	16
no. of chloride atoms	0	1
root-mean-square deviation from ideality		
bond distances (Å)	0.017	0.016
bond angles (deg)	1.486	1.518
average isotropic *B* factor		
protein	33	37
solvent	43	47

[a] Numbers in parentheses represent data for the highest-resolution shell. [b] $R_{merge} = (\Sigma_h\Sigma_i|I_h - I_{hi}|/\Sigma_h\Sigma_i I_{hi}]$, where I_h is the mean of I_{hi} observations of reflection h. [c] $R_{factor} = \Sigma||F_o| - |F_c||/\Sigma|F_o| \times 100$ for 95% of the recorded data. [d] $R_{free} = \Sigma||F_o| - |F_c||/\Sigma|F_o| \times 100$ for 5% of the recorded data.

54−56% saturated ammonium sulfate conditions within 3−5 days for the internal aldimine and with 52% saturated ammonium sulfate for the external aldimine. Larger multicrystal aggregates were broken up, mounted, and stored in liquid nitrogen using 23% ethylene glycol in mother liquor for the cryoprotectant. Data were collected on beamline 9-2 at the Stanford Synchrotron Radiation Lightsource. Diffraction data were processed with MOSFLM and scaled with SCALA.[17] Crystal parameters and data collection statistics are listed in Table 1.

Structure Determination and Refinement. Both the internal and external aldimine structures were determined by molecular replacement using *E. coli* AAT [Protein Data Bank (PDB) entry 1ASE] as the search model.[18] Model building was performed with COOT.[19] Refinement, including TLS parametrization, employed REFMAC[20] first and then Phenix.[21] Both the internal aldimine (as a modified Lys258 residue, 3QN) and the external aldimine (3QP, built with Sketcher[17]) were added after initial refinement of the protein structure. Water, sulfate, and ethylene glycol molecules were added using COOT. The final refinement in Phenix included hydrogens. Individual isotropic *B* factors were refined for all atoms, resulting in decreased R_{factor} and R_{free} parameters. Group occupancies were refined for residues with multiple conformations, as well as waters, sulfates, and ethylene glycols. The TLS refinement used three groups of residues (13−54, 55−330, and 331−408) determined from the TLS Motion Determination server (http://skuld.bmsc.washington.edu/~tlsmd/). Refinement statistics for the final structures are listed in Table 1. All structure superimpositions and images were made using CCP4Molecular Graphics.[22] The coordinates for wild-type AAT reconstituted with deazaPLP have been deposited in the Protein Data Bank (entry 3QN6 for the internal aldimine and entry 3QPG for the L-aspartate external aldimine).

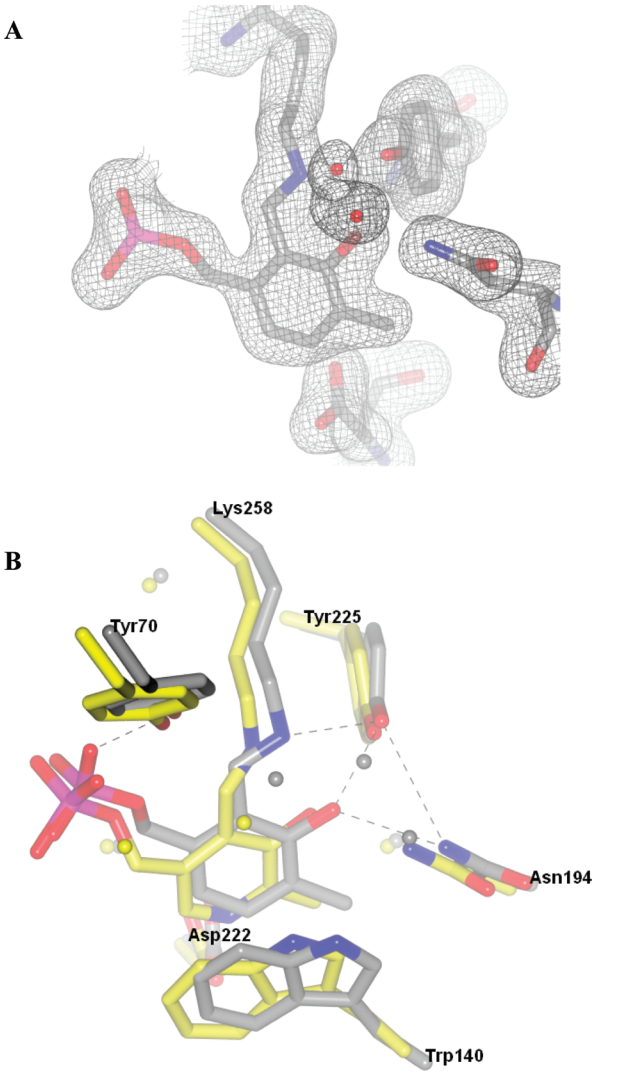

Figure 2. (A) $2F_o - F_c$ electron density map (1σ) of the deazaPLP internal aldimine. (B) Overlay of the active site of the deazaPLP (gray) and PLP (yellow) active sites (PDB entry 1AJR).

RESULTS

Overall Structure of the DeazaPLP Internal Aldimine. Aspartate aminotranferase exists in solution as an α_2 dimer with each subunit composed of 396 amino acid residues. In the $C222_1$ space group obtained here, the asymmetric unit consists of one

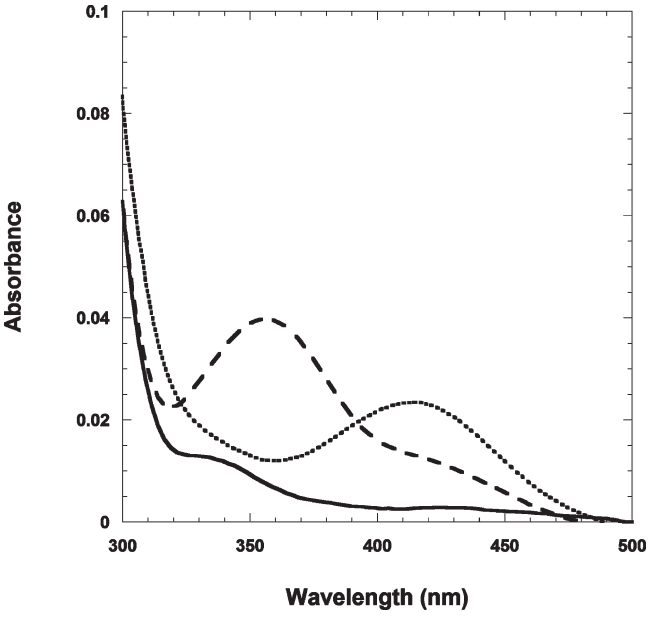

Figure 3. UV−vis spectra of apo AAT (—) AAT·PLP, (– – –), and AAT·deazaPLP (■■■). Conditions: 100 mM TEA, pH 8.0, and ∼5 μM enzyme.

monomer of this dimer. Ramachandran plots show all residues within acceptable regions except Tyr161, Ser296, and Asn347, which are marginal but were confirmed to have the correct conformation. Superimposition of the final refined internal aldimine model with the coordinates (PDB entry 1ASE) of the structure used for phasing[18] resulted in a root-mean-square deviation (rmsd) of 1.0 Å for 392 equivalent α-carbons. The greatest difference was found in residues 1−46 with displacements of 1.2−3.7 Å. Other displacements greater than 2 Å include those of Gly345, Asn347, Glu375, and Glu376. Each subunit consists of two domains: a small domain (residues 1−48 and 326−396) and a large, PLP-binding domain.[23] The domains consist of the following secondary structures: two pairs of β-strands (one parallel and the other antiparallel) and five α-helices in the small domain and 12 - helices, one of which is shared with the small domain, and a central seven-strand β-sheet, with one strand antiparallel, in the large domain.[23] The subunit interface, as previously detailed,[23] is required for formation of the two active sites, each one binding one deazaPLP cofactor and consisting of residues from each subunit.

Active Site of the DeazaPLP Internal Aldimine. Panels A and B of Figure 2 show the $2F_o - F_c$ electron density map of the active site and its overlay with the PLP internal aldimine, respectively (PDB entry 1AJR, a pig cytosolic structure at low pH). The internal aldimine is formed between the C4′ aldehyde of the deazaPLP cofactor and the ε-amino group of Lys258 (see Figure 1A for numbering). The Schiff base is nearly coplanar to the pyridine ring, with a torsion angle of ∼7°. It displays maximal absorbance at ∼420 nm in solution,[14] consistent with a protonated aldimine[24] (Figure 3). The O3′ phenol of deazaPLP forms a hydrogen bond to both Tyr225 and the side chain amide nitrogen of Asn194. The phosphate moiety of the cofactor accepts a total of nine hydrogen bonds from the following donors: the alcohol and main chain amide of Thr109, the side chain of Arg266, the phenol of Tyr70, the alcohol of Ser257, the main chain amide of Gly108, and the alcohol of Ser255. Asp222,

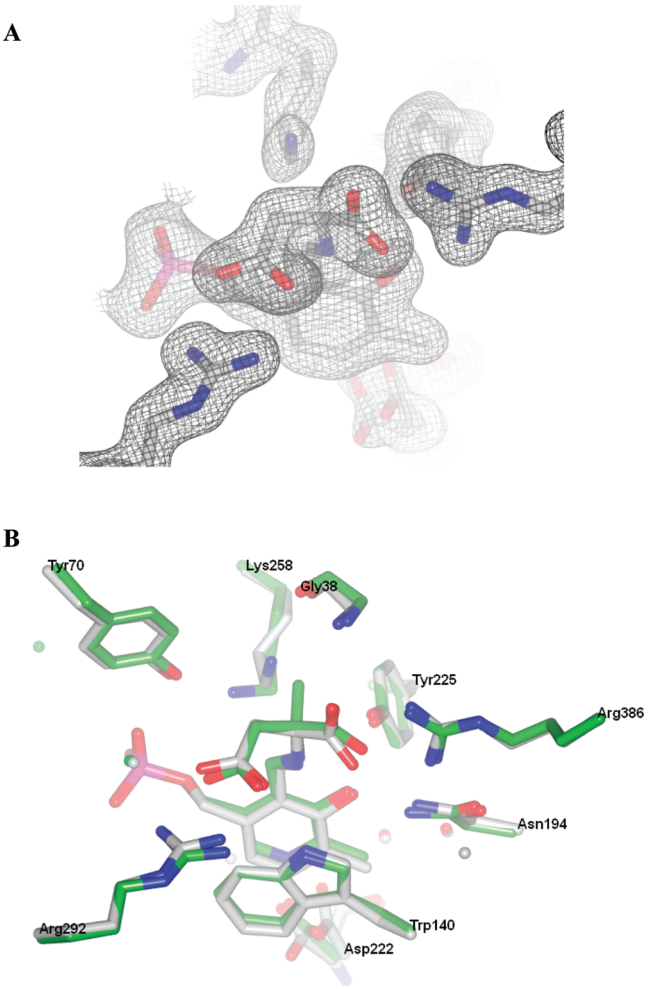

Figure 4. (A) $2F_o - F_c$ electron density map (1σ) of the deazaPLP·L-aspartate external aldimine. (B) Overlay of the α-methyl-L-aspartate·PLP external aldimine[23] (green) and the L-aspartate·deazaPLP external aldimine (light gray) active sites (PDB entry 1ART).

normally forming a salt bridge to the pyridine nitrogen of PLP,[8] is hydrogen bonded to the main chain amide of Ala224 and two water molecules, one unique to the deazaPLP structure and the other water present in PDB entry 1AJR.

Overall Structure of the L-Aspartate·DeazaPLP External Aldimine. As with the deazaPLP internal aldimine, Ramachandran plots show all residues within acceptable regions except for Tyr161, Ser296, and Asn347, which were confirmed to have correct conformations. Superimposition of the final refined model with the coordinates (PDB entry 1ASE) used for phase determination[18] results in a fit with an rmsd of 0.37 Å for 395 equivalent α-carbons. Four residues had a displacement of >1 Å: Asn347, Arg348, Asp349, and Ser363. When the substrate binds, the small domain moves ∼5°[23] toward the large domain, resulting in a transition from the "open" internal aldimine to the "closed" external aldimine structure. The secondary structure, as previously noted, is essentially identical for both the open and closed forms.[23]

Active Site of the L-Aspartate·DeazaPLP External Aldimine. Figure 4A shows the $2F_o - F_c$ electron density map of the active site, and Figure 5 shows the active site residues of the L-aspartate·deazaPLP external aldimine. The Schiff base has a

dx.doi.org/10.1021/bi200436y |*Biochemistry* 2011, 50, 5918–5924

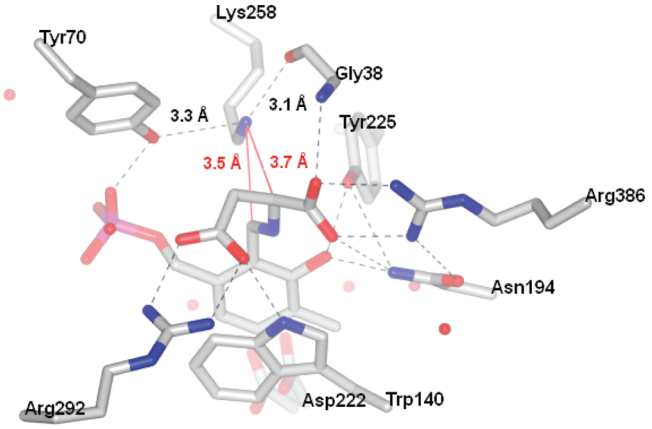

Figure 5. Active site of the deazaPLP·L-aspartate external aldimine with hydrogen bonds (dashed lines) and distances (red) from the ε-amino group of Lys258 to Cα of L-aspartate and C4′ of the cofactor analogue.

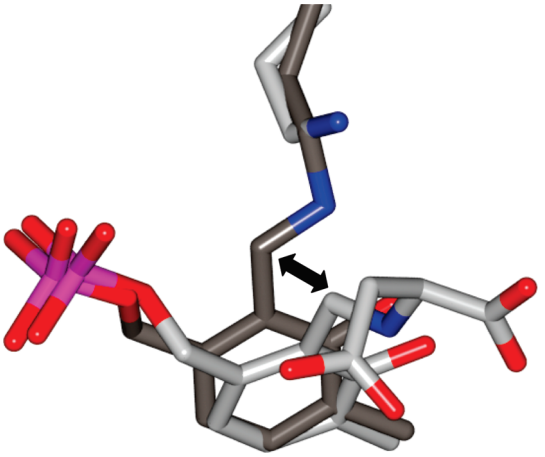

Figure 6. Overlay of the deazaPLP internal aldimine (dark gray) and the deazaPLP·L-aspartate external aldimine (light gray) showing cofactor tilt toward the substrate upon formation of the external aldimine.

torsion angle of −57° relative to the plane of the pyridine ring. The ε-amino group of Lys258, the catalytic base for the 1,3-prototropic shift central to transamination, is hydrogen bonded to the main chain carbonyl oxygen of Gly38. The distances from the ε-amino group of Lys258 to Cα of L-aspartate and C4′ of the cofactor analogue are 3.7 and 3.5 Å, respectively. The α-carboxylate oxygens of L-aspartate accept three hydrogen bonds: two from Arg386 and one from the side chain amide of Asn194. The β-carboxylate oxygens of L-aspartate accept four hydrogen bonds: two from Arg292, one from the indole nitrogen of Trp140, and one from a water. Asp222 forms hydrogen bonds to the side chain of His143, a water, and the main chain amide of Ala224.

Comparison of the PLP and DeazaPLP Internal and External Aldimines. Figure 3B shows the active site superimpositions of the internal aldimines of deazaPLP and PLP (PDB entry 1AJR). Figure 4B shows the superimposition of the active sites of the L-aspartate·deazaPLP and α-methyl-L-asparate·PLP (PDB entry 1ART) external aldimines. The rmsd values of the superimpositions are 1.17 for the internal aldimines and 0.38 for the external aldimines (390 and 396 equivalent α-carbons, respectively). Figure 6 shows the superimposition of deazaPLP in the internal and external aldimine forms to emphasize changes in the cofactor tilt upon formation of the external aldimine.

DISCUSSION

The overall structures of the internal and external aldimine forms reported here are very similar to those previously reported.[23] There are no significant differences in secondary or tertiary structure, with changes localized to the active site being the only significant ones.

The active sites of the deazaPLP internal and external aldimines of AAT are very similar to those of their respective PLP aldimines (Figures 2B and 4B, respectively). The active site residues of the deazaPLP internal aldimine shows some minor changes with respect to the PLP internal aldimine: the hydrogen bonding of the phosphate moiety differs from that of the PLP internal aldimine in that a hydrogen bond to water is replaced by a second one to Ser257 and the side chain of Arg292 of the deazaPLP internal aldimine is oriented as found in the closed conformation.[23] Tyr225 and Asn194 are identical in orientation in the deazaPLP and PLP internal aldimines.

The orientation of deazaPLP itself in the internal aldimine structure does show some significant changes with respect to PLP. Most notably, the internal aldimine Schiff base linkage between Lys258 and C4′ of deazaPLP is nearly coplanar with the pyridine ring, with a 7° dihedral angle compared to an ∼35° angle for PLP (Figure 2B). The relaxed conformation of the Schiff base with deazaPLP is reminiscent of the orientation of the Schiff base in the PLP internal aldimine of D222A AAT.[25] In D222A AAT, the unprotonated pyridine N, with diminished electrophilicity, would result in greater negative charge at O3′ and an increased level of interaction between it and the protonated Schiff base nitrogen. This, coupled with the loss of Asp222 as an anchor point,[25] results in the more coplanar orientation of the aldimine bond with respect to the pyridine ring. It has been estimated that the catalytic advantage of maintaining a strained internal aldimine conformation in AAT is a decrease in activation free energy by ∼16 kJ/mol through ground state destabilization, thereby increasing k_{cat}/K_m by ∼10^3.[25] Lastly, as with D222A,[26] no change in the ionization state of the internal aldimine in deazaPLP AAT is observed between pH 7 and 10, as indicated by the unaltered 420 nm absorption band of the internal aldimine across this pH range (data not shown). This indicates a high pK_a (>10) for the Schiff base.

The L-aspartate/deazaPLP external aldimine is gratifyingly similar in structure to its α-methyl-L-aspartate/PLP counterpart. As seen in Figure 6, deazaPLP AAT undergoes a large cofactor tilt upon formation of the external aldimine. A similar but less pronounced tilt occurs upon formation of the external aldimine with the PLP form of AAT.[23] In both cases, there is a movement of the cofactor away from Lys258, toward the dicarboxylate substrate. This orients the pyridine ring more planar with the Trp140 indole group. The internal to external aldimine conversion results in an ∼17° tilt toward substrate for PLP[23] and ∼26° for deazaPLP.

The most mechanistically important difference centers on the ε-amino group of Lys258, the catalytic base for the 1,3-prototropic shift between Cα and C4′.[27] In the α-methyl-L-aspartate structure, the ε-amino group of Lys258 is hydrogen bonded to Tyr70,[23] while the steric bulk of the α-methyl group precludes it

from being oriented over Cα, which would be required for deprotonation. On the other hand, the ε-amino group of Lys258 in the L-aspartate·deazaPLP external aldimine is hydrogen bonded to the backbone carbonyl oxygen of Gly38 and sits directly over the aldimine linkage. It is nearly equidistant between C4′ (3.5 Å) and Cα (3.7 Å), which participate in the central 1,3-prototropic shift. The hydrogen bond to Tyr70 is maintained, but its length is increased by 0.6 Å[23] in the deazaPLP external aldimine. The role Gly38 plays in orienting the ε-amino group of Lys258 has not been addressed in previous work detailing the mechanism of AAT.[27] Instead, Tyr70 was proposed to be the residue primarily involved. However, Gly38 was previously implicated as a possible hydrogen bond acceptor for water in ketimine hydrolysis.[27] Gly38 is completely conserved in the first 500 sequences returned with a BLAST search of the NCBI nonredundant protein sequence database using the *E. coli* AAT sequence with default parameters.

No detectable reaction of deazaPLP AAT with L-aspartate as a substrate was observed over ∼2 days in solution (unpublished results), a truly remarkable result given that the L-aspartate·deazaPLP external aldimine in AAT is catalytically primed from a structural perspective. While a decrease in activity at least on par with that seen with D222A (∼10^5-fold decrease; half-life of ∼10 min)[8] would be expected with deazaPLP, the absence of the pyridine nitrogen proves additionally detrimental. The half-life of the reaction of deazaPLP AAT with L-aspartate is estimated to be >20 days, which corresponds to a >10^9-fold decrease in reactivity compared to that of PLP AAT. The half-life of deazaPLP AAT with the activated substrate L-cysteine sulfinate is ∼38 h (unpublished results), which is ∼10^8-fold shorter than that of the corresponding PLP AAT reaction. These results indicate that the pyridine nitrogen of PLP is more important to AAT catalysis than even Lys258, the acid/base catalyst, because the K258A mutant results in an ∼10^8-fold decrease in reactivity with L-aspartate.[16]

The inactivity observed with deazaPLP-reconstituted AAT may be specific to transaminases that catalyze a 1,3-prototropic shift, with proton transfers at both Cα (a step common to many PLP-catalyzed reactions) and C4′. Alanine racemase, on the other hand, is a PLP enzyme that catalyzes proton transfers at Cα only and has a high fidelity (∼10^6-fold) for racemization over transamination. It maintains the pyridine nitrogen in a formally neutral state through interaction with Arg219.[1] Although no spectroscopically observable carbanionic intermediate occurs in alanine racemase, multiple kinetic isotope effects have established that the mechanism proceeds through a high-energy carbanionic intermediate.[28] Interestingly, it is precisely the instability of the carbanionic intermediate that may be responsible for the high fidelity of ALR, because transamination requires rate-limiting movement of the active site lysine or tyrosine to protonate C4′ of PLP, and this would be suppressed by the short lifetime of the quinonoid intermediate.[1] A similar observation was made with D-amino acid transaminase, which protonates the pyridine nitrogen via Glu177. In the E177K mutant, the extent of transamination is decreased by 1000-fold while that of racemization is increased 10-fold.[11] Finally, OASS is a fold-type II PLP enzyme that catalyzes the β-elimination of acetate from *O*-acetyl-L-serine and probably maintains the pyridine nitrogen in an unprotonated state via hydrogen bonding with Ser272. As in the ALR-catalyzed reaction, buildup of negative charge at C4′ in a carbanionic intermediate would be counterproductive because it would both discourage leaving group elimination and promote the transamination side reaction. Cook[29] has suggested that the OASS reaction mechanism does not include a carbanionic intermediate. Rather, elimination is proposed to occur via an E2-type concerted β-elimination of acetate, a good leaving group, which would not require substantial stabilization of a carbanionic intermediate by a protonated pyridine ring.

The discussion given above suggests that PLP enzymes may partially control the fate of the carbanionic intermediate by modulating the extent of positive charge on the pyridine ring. Recent computational studies show that pyridine nitrogen protonation facilitates protonation of the carbanionic intermediate at C4′ compared to Cα.[13] This is further supported by a recent study of substituent effects on the carbonyl-catalyzed deprotonation of the Cα-H of glycine.[30] Formation of a Schiff base between 5′-deoxypyridoxal (neutral pyridine nitrogen) and glycine causes a decrease in the pK_a of the Cα-H of glycine from ∼29 (pK_a for free amino acid) to ∼23. The Schiff base between 5′-deoxypyridoxal (protonated pyridine nitrogen) and glycine results in a pK_a of ∼17. Crugeiras et al. argue that the greater acidity of the Cα proton of glycine in the Schiff base with the protonated form of 5′-deoxypyridoxal provides direct evidence of stronger delocalization of negative charge with the π-electron system that, in turn, would favor the 1,3-prototropic shift central to transamination.[30] Lastly, salicylaldehydes have been observed to catalyze the racemization of amino acids but not their transamination, demonstrating that the carbanion formed has a strong preference for protonation at Cα.[31,32]

AUTHOR INFORMATION

Corresponding Author

*Telephone: (530) 754-5282. Fax: (530) 752-8995. E-mail: mdtoney@ucdavis.edu.

ABBREVIATIONS

AAT, aspartate aminotransferase; ALR, alanine racemase; OASS, *O*-acetylserine sulfhydrylase; PLP, pyridoxal 5′-phosphate; deazaPLP, 1-deazapyridoxal 5′-phosphate; TEA, triethanolamine; LB, Luria-Bertani broth.

REFERENCES

(1) Toney, M. D. (2005) Reaction specificity in pyridoxal phosphate enzymes. *Arch. Biochem. Biophys. 433*, 279–287.

(2) Eliot, A. C., and Kirsch, J. F. (2004) Pyridoxal phosphate enzymes: Mechanistic, structural, and evolutionary considerations. *Annu. Rev. Biochem. 73*, 383–415.

(3) Hayashi, H. (1995) Pyridoxal enzymes: Mechanistic diversity and uniformity. *J. Biochem. 118*, 463–473.

(4) Hyde, C. C., Ahmed, S. A., Padlan, E. A., Miles, E. W., and Davies, D. R. (1988) Three-dimensional structure of the trptophan synthase α2β2 multienzyme complex from *Salmonella typhimurium*. *J. Biol. Chem. 263*, 17857–17871.

(5) Shaw, J. P., Petsko, G. A., and Ringe, D. (1997) Determination of the structure of alanine racemase from *Bacillus stearothermophilus* at 1.9-Å resolution. *Biochemistry 36*, 1329–1342.

(6) Burkhard, P., Rao, G. S., Hohenester, E., Schnackerz, K. D., Cook, P. F., and Jansonius, J. N. (1998) Three-dimensional structure of O-acetylserine sulfhydrylase from *Salmonella typhimurium*. *J. Mol. Biol. 283*, 121–133.

(7) Zabinski, R. F., and Toney, M. D. (2001) Metal ion inhibition of nonenzymatic pyridoxal phosphate catalyzed decarboxylation and transamination. *J. Am. Chem. Soc. 123*, 193–198.

(8) Onuffer, J. J., and Kirsch, J. F. (1994) Characterization of the apparent negative co-operativity induced in *Escherichia coli* aspartate aminotransferase by the replacement of Asp222 with alanine. Evidence for an extremely slow conformational change. *Protein Eng. 7*, 413–424.

(9) Sharif, S., Fogle, E., Toney, M. D., Denisov, G. S., Shenderovich, I. G., Buntkowsky, G., Tolstoy, P. M., Huot, M. C., and Limbach, H. H. (2007) NMR localization of protons in critical enzyme hydrogen bonds. *J. Am. Chem. Soc. 129*, 9558–9559.

(10) Bach, R. D., Canepa, C., and Glukhovtsev, M. N. (1999) Influence of Electrostatic Effects on Activation Barriers in Enzymatic Reactions: Pyridoxal 5′-Phosphate-Dependent Decarboxylation of α-Amino Acids. *J. Am. Chem. Soc. 121*, 6542–6555.

(11) Richard, J. P., Amyes, T. L., Crugeiras, J., and Rios, A. (2009) Pyridoxal 5′-phosphate: Electrophilic catalyst extraordinaire. *Curr. Opin. Chem. Biol. 13*, 475–483.

(12) Major, D. T., Nam, K., and Gao, J. (2006) Transition state stabilization and α-amino carbon acidity in alanine racemase. *J. Am. Chem. Soc. 128*, 8114–8115.

(13) Casasnovas, R., Salva, A., Frau, J., Donoso, J., and Munoz, F. (2009) Theoretical study on the distribution of atomic charges in the Schiff bases of 3-hydroxypyridine-4-aldehyde and alanine. The effect of the protonation state of the pyridine and imine nitrogen atoms. *Chem. Phys. 355*, 149–156.

(14) Griswold, W. R., and Toney, M. D. (2010) Chemoenzymatic synthesis of 1-deaza-pyridoxal 5′-phosphate. *Bioorg. Med. Chem. Lett. 20*, 1352–1354.

(15) Vieira, J., and Messing, J. (1987) Production of single-stranded plasmid DNA. *Methods Enzymol. 153*, 3–11.

(16) Toney, M. D., and Kirsch, J. F. (1993) Lysine 258 in aspartate aminotransferase: Enforcer of the Circe effect for amino acid substrates and general-base catalyst for the 1,3-prototropic shift. *Biochemistry 32*, 1471–1479.

(17) Collaborative Computational Project Numer 4. (1994) The ccp4 suite: Programs for protein crystallography. *Acta Crystallogr. D50*, 760–763.

(18) Schumacher, C., and Ringe, D. (1994) The structure of wild-type *E. coli* aspartate aminotransferse reconstituted with PLP-N-Oxide, Protein Data Bank entry 1ASE.

(19) Emsley, P., and Cowtan, K. (2004) Coot: Model-building tools for molecular graphics. *Acta Crystallogr. D60*, 2126–2132.

(20) Murshudov, G. N., Vagin, A. A., and Dodson, E. J. (1997) Refinement of macromolecular structures by the maximum-likelihood method. *Acta Crystallogr. D53*, 240–255 .

(21) Afonine, P. V., Grosse-Kunstleve, R. W., and Adams, P. D. (2005) *CCP4 Newsletter*, Vol. 42, Contribution 8.

(22) Potterton, E., McNicholas, S., Krissinel, E., Cowtan, K., and Noble, M. (2002) The CCP4 molecular-graphics project. *Acta Crystallogr. D58*, 1955–1957.

(23) Okamoto, A., Higuchi, T., Hirotsu, K., Kuramitsu, S., and Kagamiyama, H. (1994) X-ray crystallographic study of pyridoxal 5′-phosphate-type aspartate aminotransferases from *Escherichia coli* in open and closed form. *J. Biochem. 116*, 95–107.

(24) Hayashi, H., Mizuguchi, H., and Kagamiyama, H. (1998) The imine-pyridine torsion of the pyridoxal 5′-phosphate Schiff base of aspartate aminotransferase lowers its pKa in the unliganded enzyme and is crucial for the successive increase in the pKa during catalysis. *Biochemistry 37*, 15076–15085.

(25) Hayashi, H., Mizuguchi, H., Miyahara, I., Islam, M. M., Ikushiro, H., Nakajima, Y., Hirotsu, K., and Kagamiyama, H. (2003) Strain and catalysis in aspartate aminotransferase. *Biochim. Biophys. Acta 1647*, 103–109.

(26) Yano, T., Kuramitsu, S., Tanase, S., Morino, Y., and Kagamiyama, H. (1992) Role of Asp222 in the catalytic mechanism of *Escherichia coli* aspartate aminotransferase: The amino acid residue which enhances the function of the enzyme-bound coenzyme pyridoxal 5′-phosphate. *Biochemistry 31*, 5878–5887.

(27) Kirsch, J. F., Eichele, G., Ford, G. C., Vincent, M. G., Jansonius, J. N., Gehring, H., and Christen, P. (1984) Mechanism of action of aspartate aminotransferase proposed on the basis of its spatial structure. *J. Mol. Biol. 174*, 497–525.

(28) Spies, M. A., and Toney, M. D. (2003) Multiple hydrogen kinetic isotope effects for enzymes catalyzing exchange with solvent: Application to alanine racemase. *Biochemistry 42*, 5099–5107.

(29) Cook, P. F. (2003) α,β-Elimination reaction of O-acetylserine sulfhydrylase. Is the pyridine ring required?. *Biochim. Biophys. Acta 1647*, 66–69.

(30) Crugeiras, J., Rios, A., Riveiros, E., and Richard, J. P. (2011) Substituent Effects on Electrophillic Catalysis by the Carbonyl Group: Anatomy of the Rate Acceleration for PLP-Catalyzed Deprotonation of Glycine. *J. Am. Chem. Soc. 133*, 3173–3183.

(31) Ando, M. (1969) Catalytic Activities of Salicylaldehyde Derivatives. II. Kinetic Studies of the Racemization of Amino Acids. *Bull. Chem. Soc. Jpn. 42*, 2628–2631.

(32) Ando, M. (1978) Catalytic Activities of Salicylaldehdye Derivatives. VIII. Kinetic Studies of the Catalytic Racemization of L-Glutamic Acid at 25 °C. *Bull. Chem. Soc. Jpn. 51*, 2366–2368.